Electronic Supplementary Material (ESI) for Dalton Transactions.
This journal is © The Royal Society of Chemistry 2016

Electronic Supplementary Information (ESI) for

$[Ti_{12}In_6O_{18}(OOCC_6H_5)_{30}]$: A Multifunctional Hetero-Polyoxotitanate Nanocluster with High Stability and Visible Photoactivity

Shengjun Liu,[a,#] Wei Hu,[a,b,#] Jayanta Kr. Nath,[a] Jing Tong,[a] Xudong Hou,[a] Wenlong Liu,[d] Jinlong Yang,[c,*] and Bo Liu[a,*]

[a] Department of Chemistry, University of Science and Technology of China, Hefei, Anhui 230026, P. R. China.
[b] Computational Research Division, Lawrence Berkeley National Laboratory, Berkeley, CA 94720, USA.
[c] Hefei National Laboratory for Physical Sciences at Microscale, University of Science and Technology of China, Hefei, Anhui 230026, People's Republic of China.
[d] College of Chemistry and Chemical Engineering, Yangzhou University, Yangzhou 225002, P.R. China.
E-mail : liuchem@ustc.edu.cn; jlyang@ustc.edu.cn.

Table S1. Crystallographic data of **$POTi_{12}In_6$**.

Complex Name	$POTi_{12}In_6$
Formulae	$C_{210}H_{150}NIn_6O_{78}Ti_{12}$
CCDC No.	1451554
Mol. wt.	5207.04
Crystal system	Hexagonal
Space group	$R\bar{3}c$
Temperature (K)	296
Wavelength (Å)	0.71073
a [Å]	34.4795(17)
b [Å]	34.4795(17)
c [Å]	31.634(4)
α [°]	90.00
β [°]	90.00
γ [°]	120.00
V[Å^3]	32569(4)
Z	6
Density / gcm^{-3}	1.597
Abs.Coeff./mm^{-1}	1.094
F(000)	15676.4
Total no. of reflections	6562
Reflections, I > 2σ(I)	5173
Max. 2θ/°	25.25
Ranges (h, k, l)	-41 ≤ h ≤ 37 -34≤ k ≤ 41 -37 ≤ l ≤ 37
Complete to 2θ (%)	99
Data/Restraints/ Parameters	6562/9/464
Goof (F^2)	1.268
R indices [I > 2σ(I)]	0.0527
R indices (all data)	0.0776
WR_2 [I > 2σ(I)]	0.1727
WR_2(all data)	0.2035

Computer programs: SAINT v8.27A (Bruker, 2012), SIR2004 (Burla et al., 2007), XL (Sheldrick, 2008), OLEX2 (Dolomanov et al., 2009)

Table S2. Ti-O and In-O bond distances (Å) in the Asymmetric Unit of **$POTi_{12}In_6$** cluster.

Ti−O	Ti−O distances(Å)	In-O	In−O distances(Å)
Ti(1)-O(6)	2.00(2)	In(1)-O(2)	2.18(2)
Ti(1)-O(8)	2.08(2)	In(1)-O(3)	2.10(1)
Ti(1)-O(9)	2.04(2)	In(1)-O(5)	2.17(2)
Ti(1)-O(10)	2.05(2)	In(1)-O(7)	2.13(2)
Ti(1)-O(12)	1.86(2)	In(1)-O(12)	2.10(2)
Ti(2)-O(1)	1.98(1)		
Ti(2)-O(11)	2.02(2)		
Ti(2)-O(12)	1.94(1)		
Ti(2)-O(13)	1.90(1)		

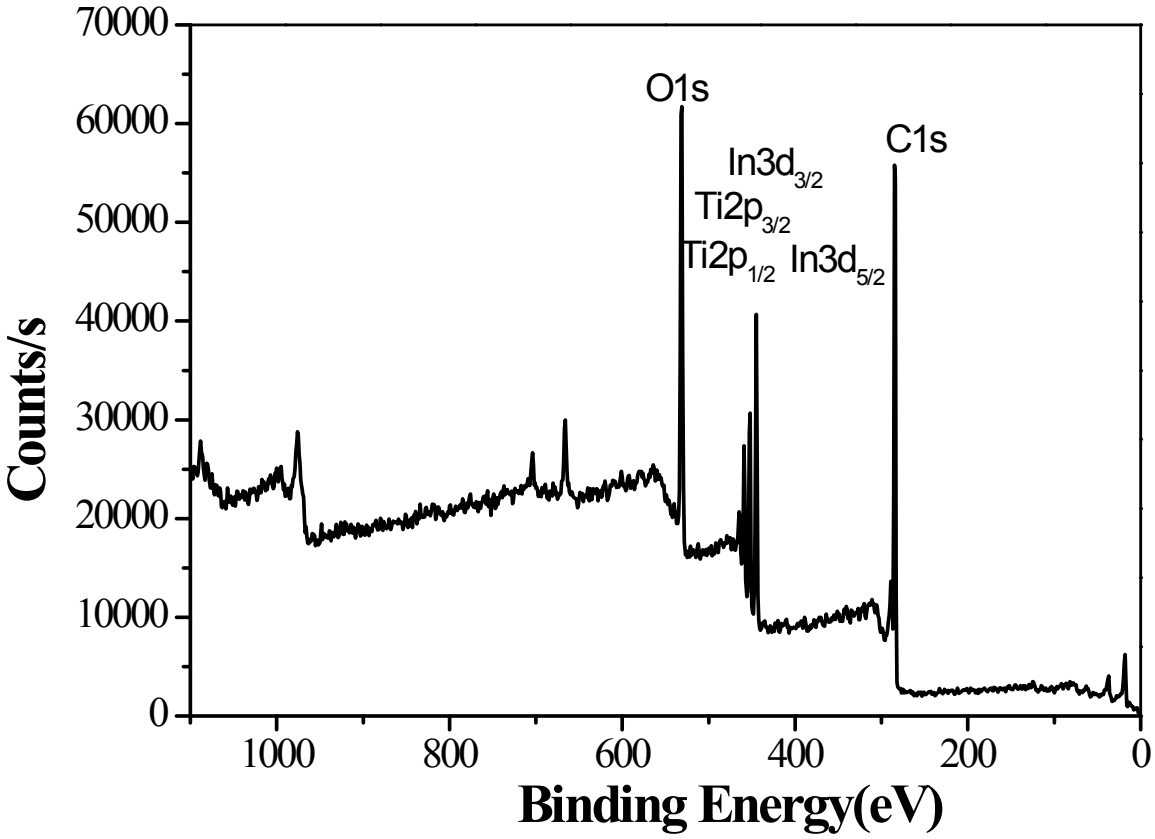

Fig. S1. X-ray photoelectron spectroscopy (XPS) survey of $\mathbf{POTi_{12}In_6}$.

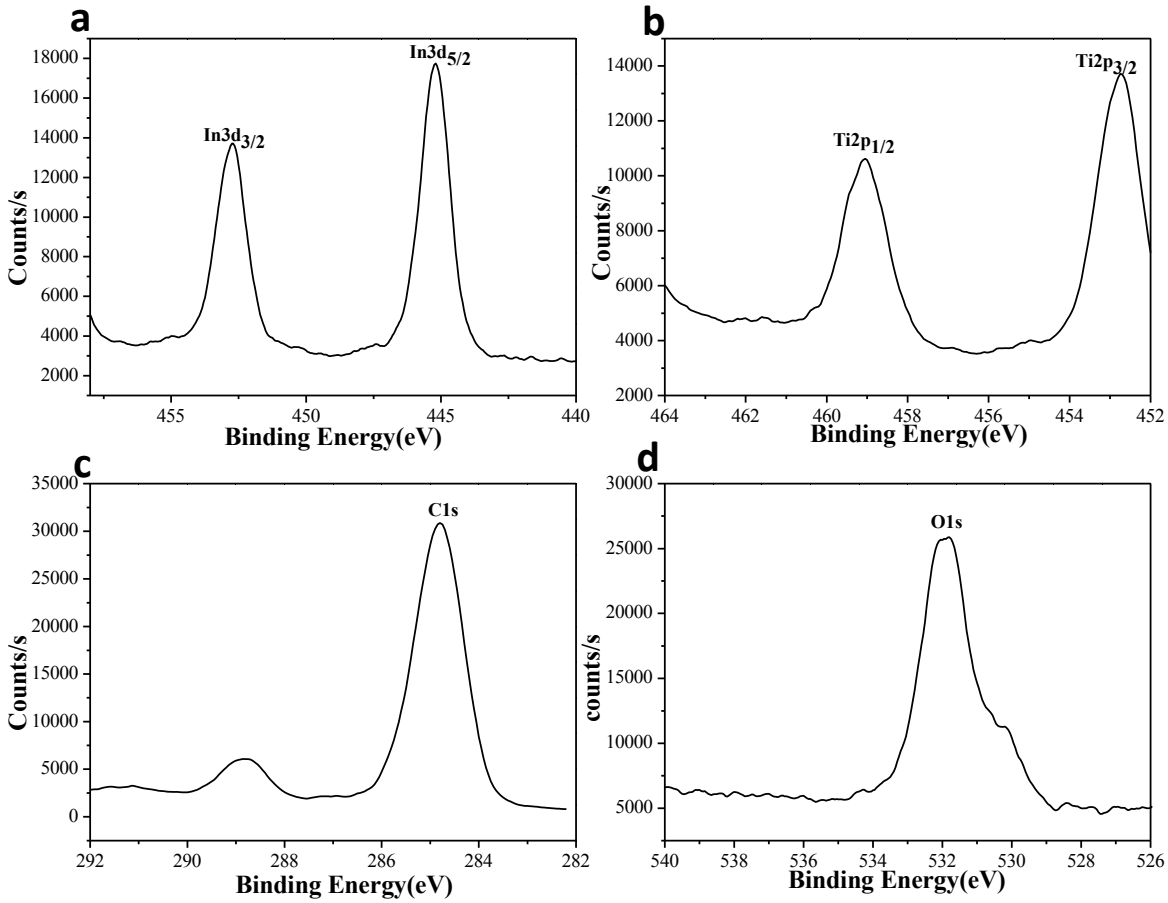

Fig. S2. XPS high-resolution spectra of In 3d, Ti 2p, C 1s and O 1s core levels for **$POTi_{12}In_6$**. (a) In 3d spectrum peaks of In $3d_{5/2}$ and In $3d_{3/2}$ with BE region centered at 445.20 and 452.70 eV, respectively, characteristics of In^{3+} oxidation state. (b) The Ti 2p spectrum shows the peaks with binding energies located at ~459.05 eV ($2p_{3/2}$) and 467.75 eV ($2p_{1/2}$), indicating titanium in Ti^{4+} oxidation state. (c) The peak with binding energy of C 1s is located at ~284.92 eV. (d) The spectrum of O 1s shown in Figure S2, reveal two peaks centered at 530.23 and 531.82 eV.

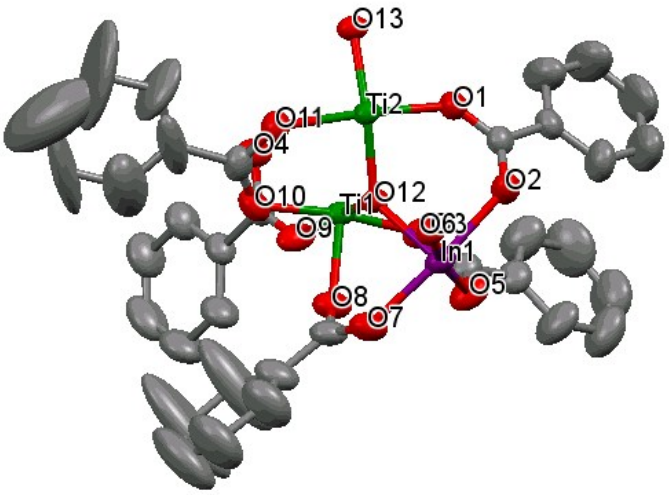

Fig. S3. Ellipsoid drawing of asymmetric unit in **$POTi_{12}In_6$**. Ti, green; In, purple; O, red and grey, carbon. Hydrogen atoms and guest molecules are omitted for clarity.

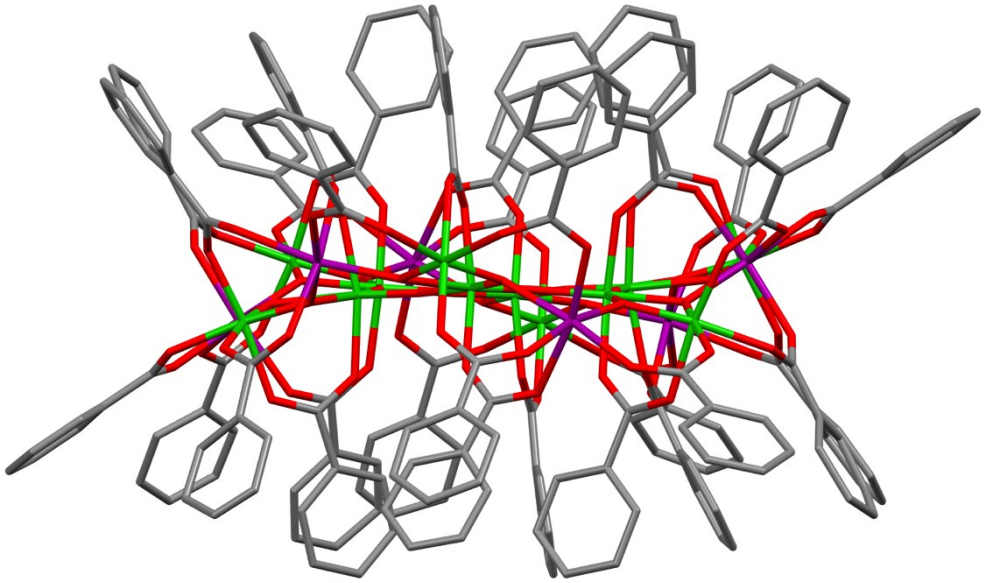

Fig. S4. Capped stick model of **$POTi_{12}In_6$** down b axis featured with a core-shell wheel structure. Ti, green: O, red; In, purple; and grey, carbon. Hydrogen atoms and lattice solvent molecules are omitted for clarity.

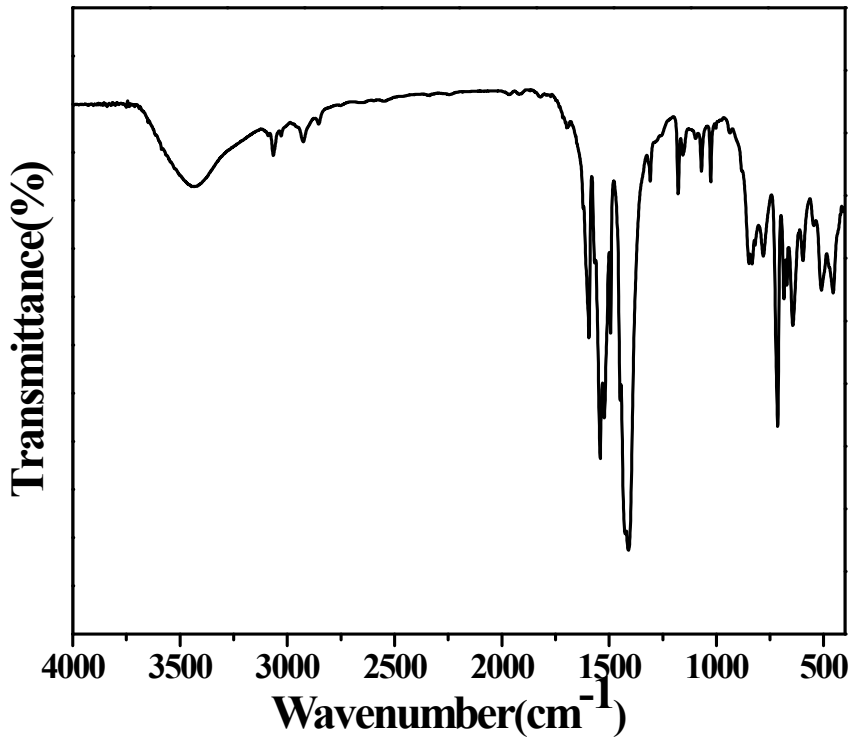

Fig. S5. Infrared spectrum of $\mathbf{POTi_{12}In_6}$: characteristic bands of the coordinated carboxylate in 1400- 1600 cm^{-1} and M-O (M = Ti, In) vibrations in 400- 800 cm^{-1}. There is no free carboxyl group vibration in 1650-1750 cm^{-1}. The broad vibration around 3500 cm^{-1} arises from water molecules.

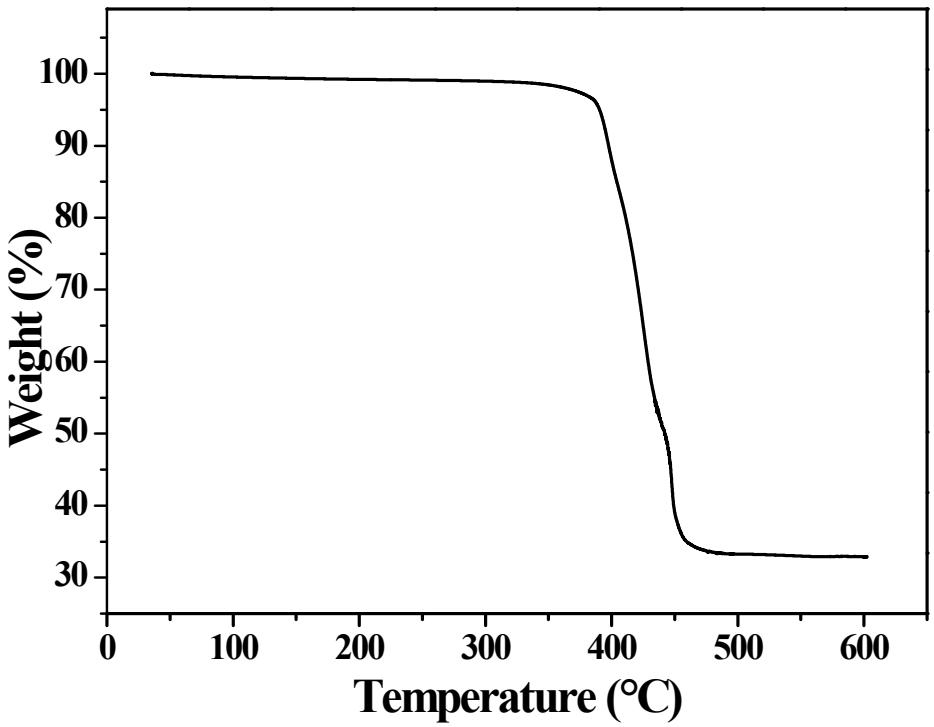

Fig. S6. TG curve of $\mathbf{POTi_{12}In_6}$ measured in air atmosphere, revealing a tiny mass loss before 120 ^{o}C due to leaving of guest acetonitrile molecules. The cluster remains intact at > 350 ^{o}C, followed by decomposition of $\mathbf{POTi_{12}In_6}$.

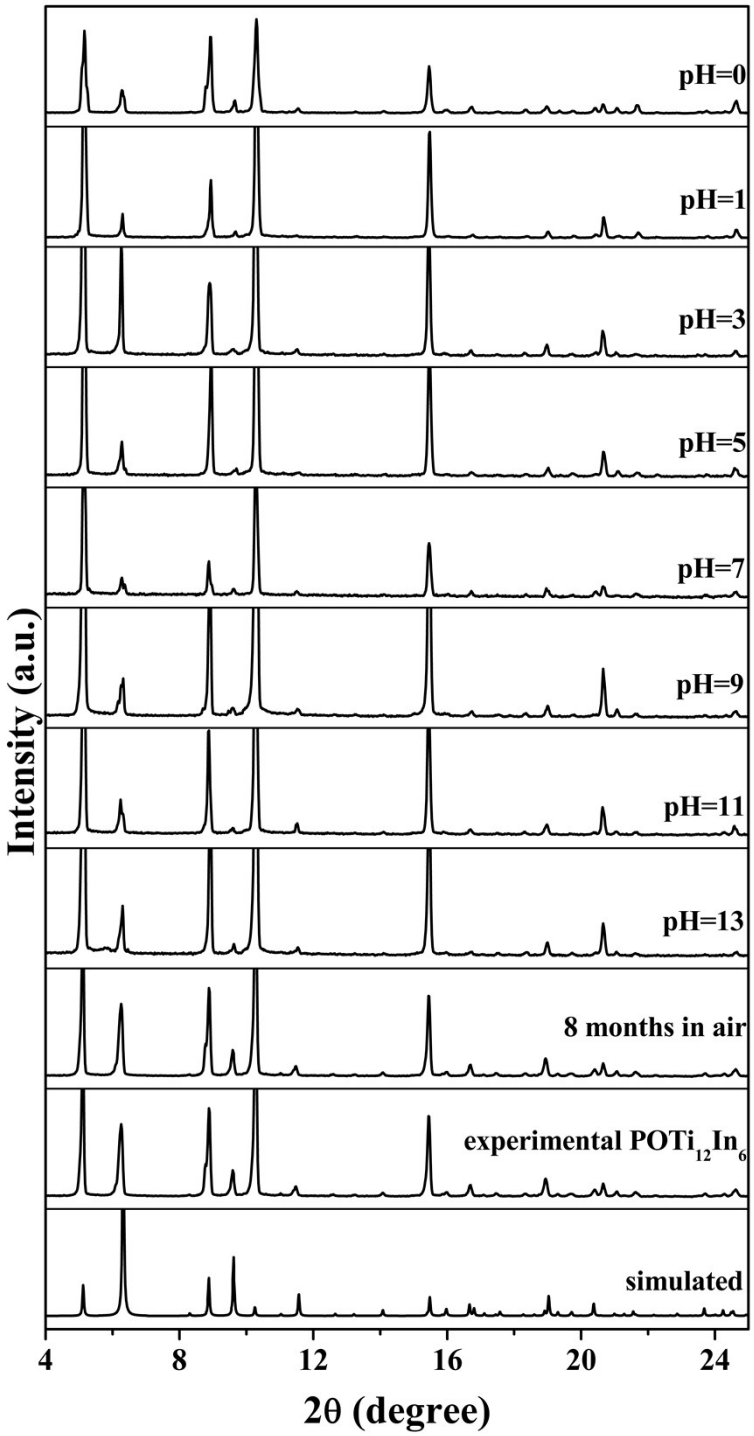

Fig. S7. Powder XRD patterns of simulated $\mathbf{POTi_{12}In_6}$, as-prepared $\mathbf{POTi_{12}In_6}$ and $\mathbf{POTi_{12}In_6}$ soaked in aqueous solution with pH value ranging from 13 to 0 for 24 hours and in air for 8 months. There is no obvious crystallinity loss under these conditions, suggesting ultrahigh stability of $\mathbf{POTi_{12}In_6}$.

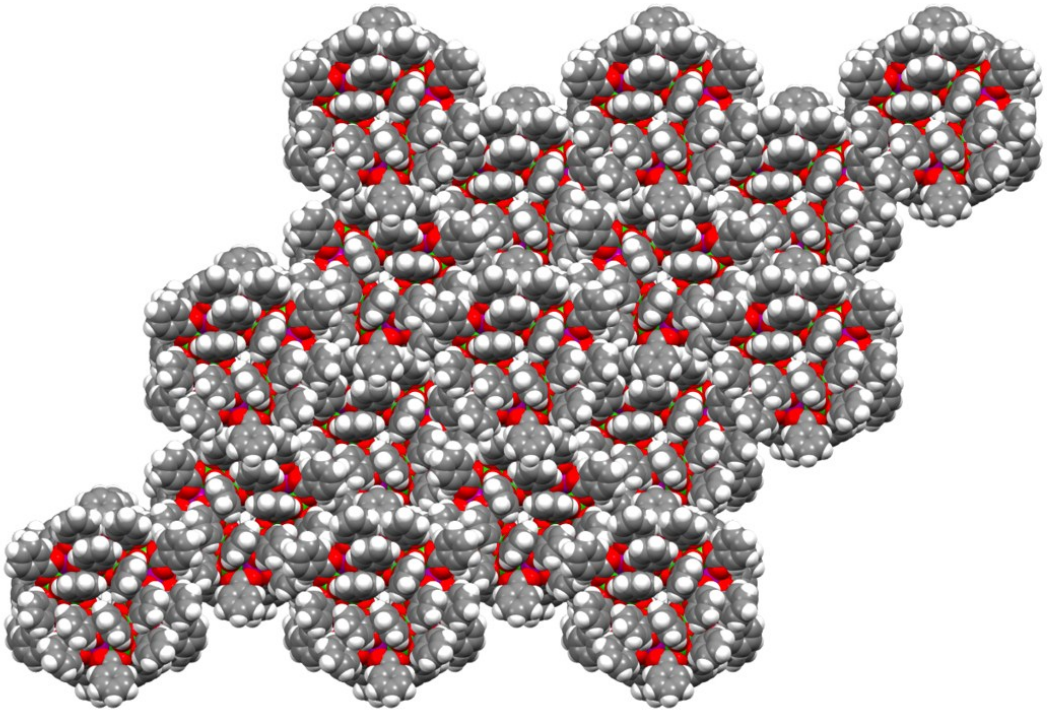

Fig. S8. Space-fill model of **$POTi_{12}In_6$** cluster, showing no intermolecular space available for guest molecule access.

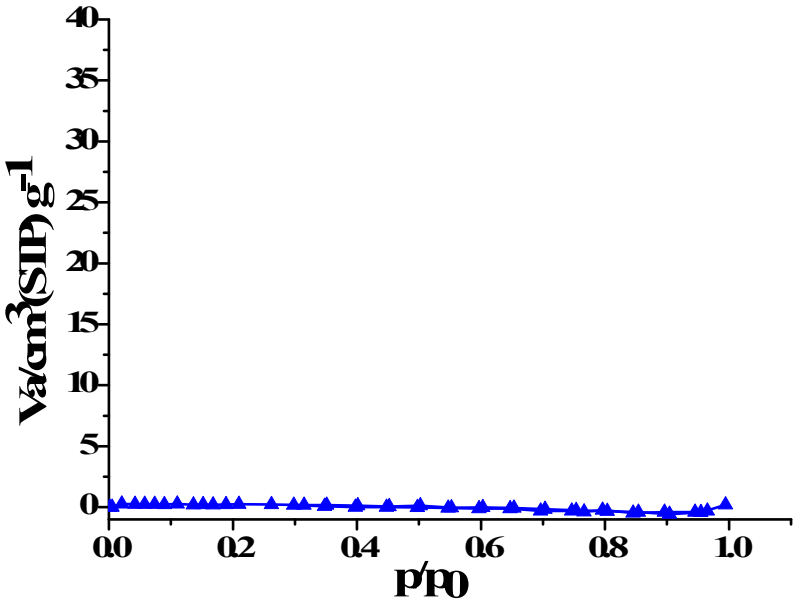

Fig. S9. N_2 sorption isotherm of **POTi$_{12}$In$_6$** at 77 K. It is noteworthy that there is some fluctuation in sorption isotherm due to very low sorption amount of N_2.

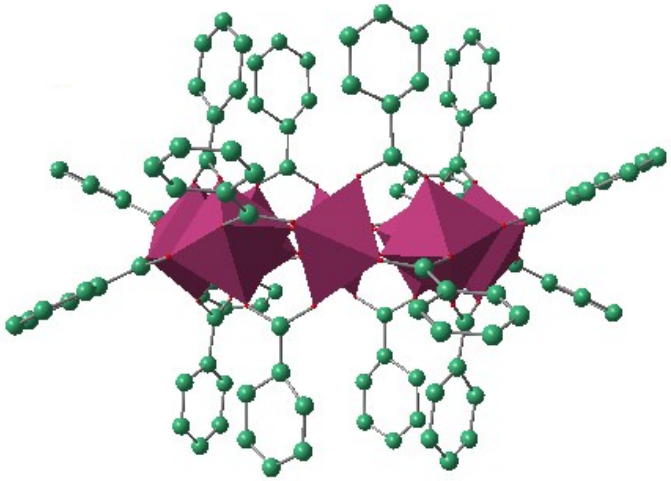

Fig. S10. Crystal structure of $Ti_8O_8(OOCC_6H_5)_{16}$(Ti_8Ph). Magenta octahedron: TiO_6, green ball: C. [1]

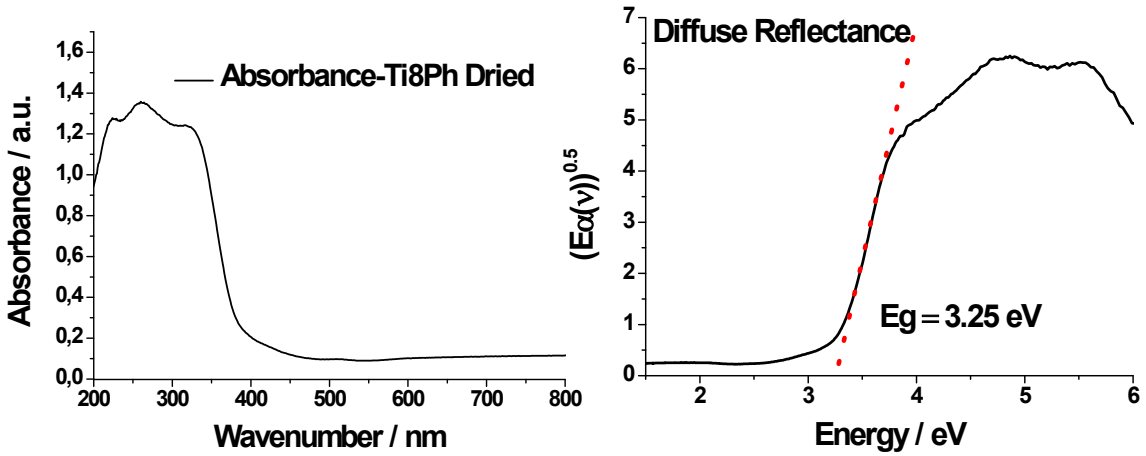

Fig. S11. UV-Visible spectrum and Tauc plot of **Ti_8Ph**.

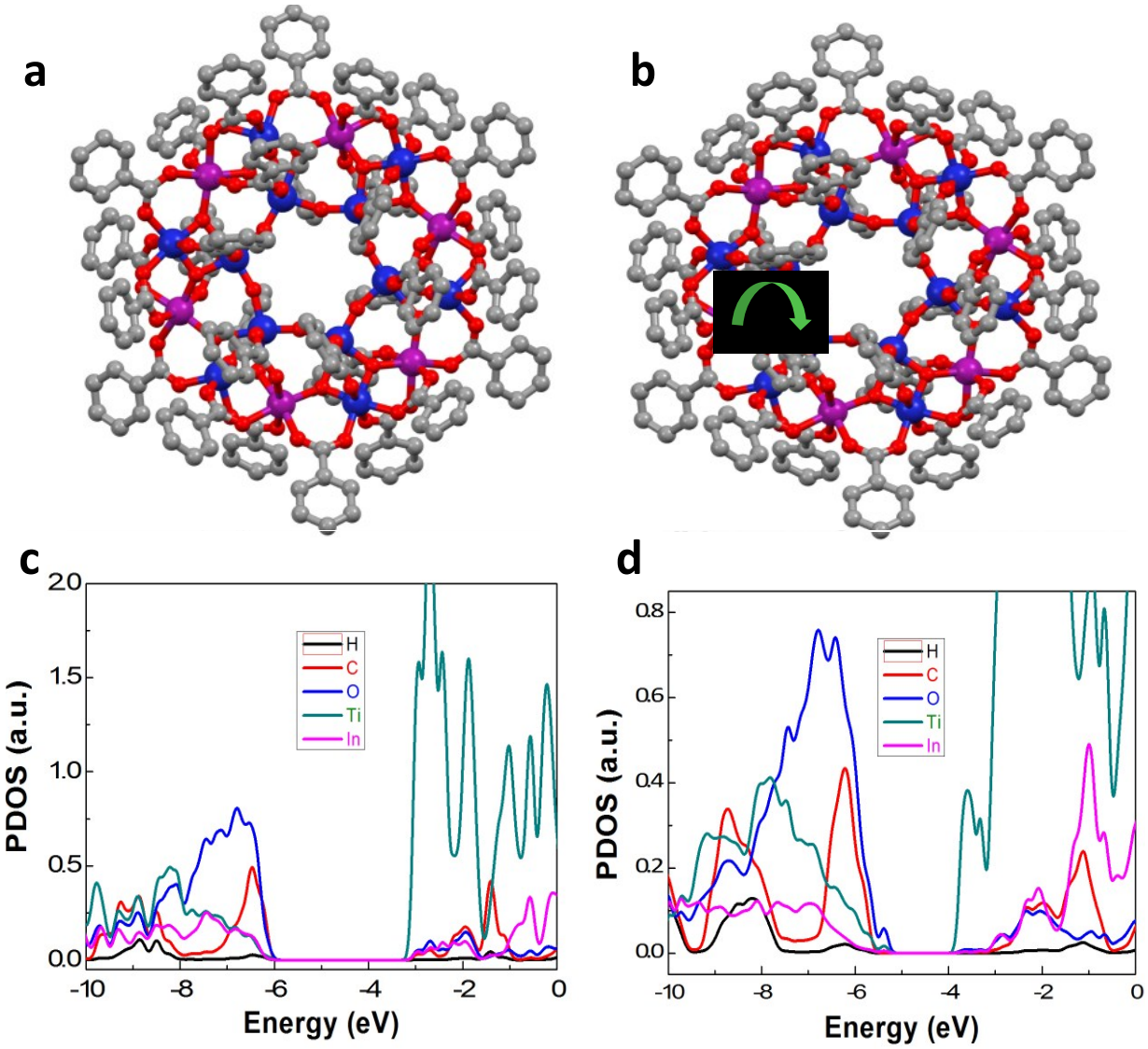

Fig. S12. Computing details of **$POTi_{12}In_6$**. Geometric structures of (a) ideal and (b) defective modes of **$POTi_{12}In_6$** cluster adopted in computing calculations. Green arrow indicates adjacent Ti and In atoms swapping. (The blue, purple, red and grey balls denote titanium, indium, oxygen and carbon atoms, respectively). Projected density of states (PDOS) per atom of (c) ideal and (d) defective **$POTi_{12}In_6$** structures.

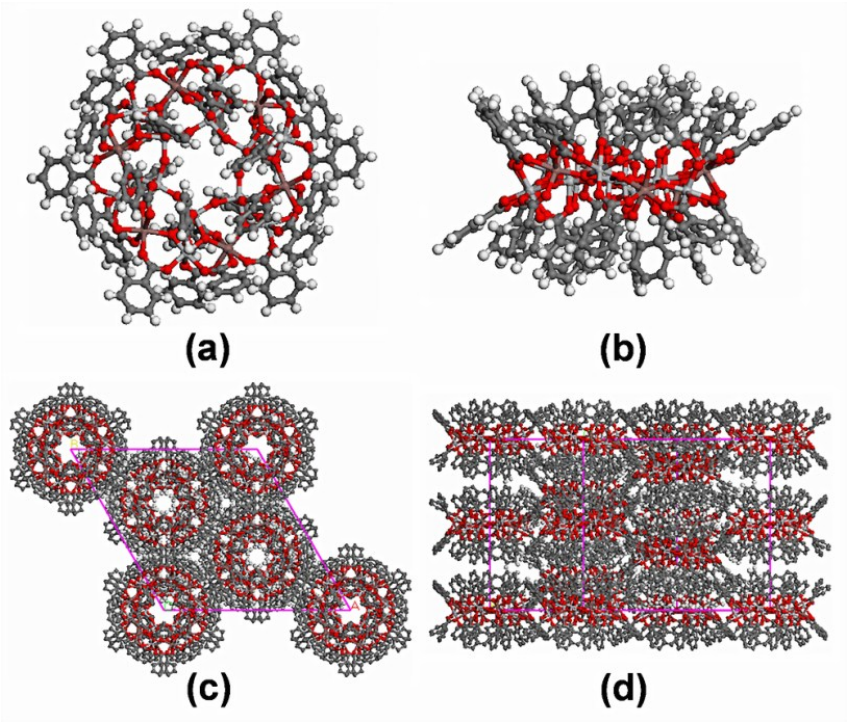

Fig. S13. Geometric structures of $\mathbf{POTi_{12}In_6}$ cluster and hexagonal periodical bulk system. (a) Top and (b) side views of $\mathbf{POTi_{12}In_6}$ cluster. (c) Top and (d) side views of bulk $\mathbf{POTi_{12}In_6}$. The silver, brown, red, gray and white balls denote titanium, indium, oxygen, carbon and hydrogen atoms, respectively. The chemical formula of $\mathbf{POTi_{12}In_6}$ cluster is $\mathbf{Ti_{12}In_6O_{78}C_{210}H_{150}}$ (456 atoms) as shown in Table S1. Bulk $\mathbf{POTi_{12}In_6}$ contains 6 $\mathbf{POTi_{12}In_6}$ clusters (2736 atoms) with the lattice parameters of a = b = 34.4795 Å, c = 31.634 Å, alpha = beta = 90.0000° and gamma = 120.000° as shown in Figure S12 (c) and (d). Guest CH_3CN molecules are ignored for calculation.

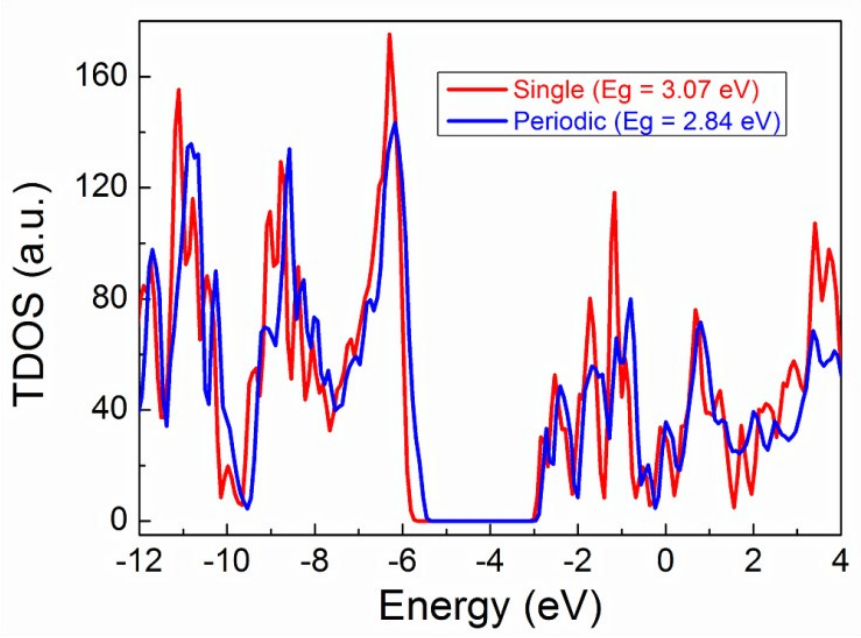

Fig. S14. Total density of states (TDOS) of $\mathbf{POTi_{12}In_6}$ cluster and hexagonal periodical bulk system. The TDOS of bulk $\mathbf{POTi_{12}In_6}$ containing 6 $\mathbf{POTi_{12}In_6}$ clusters is only shown 1/6 here.

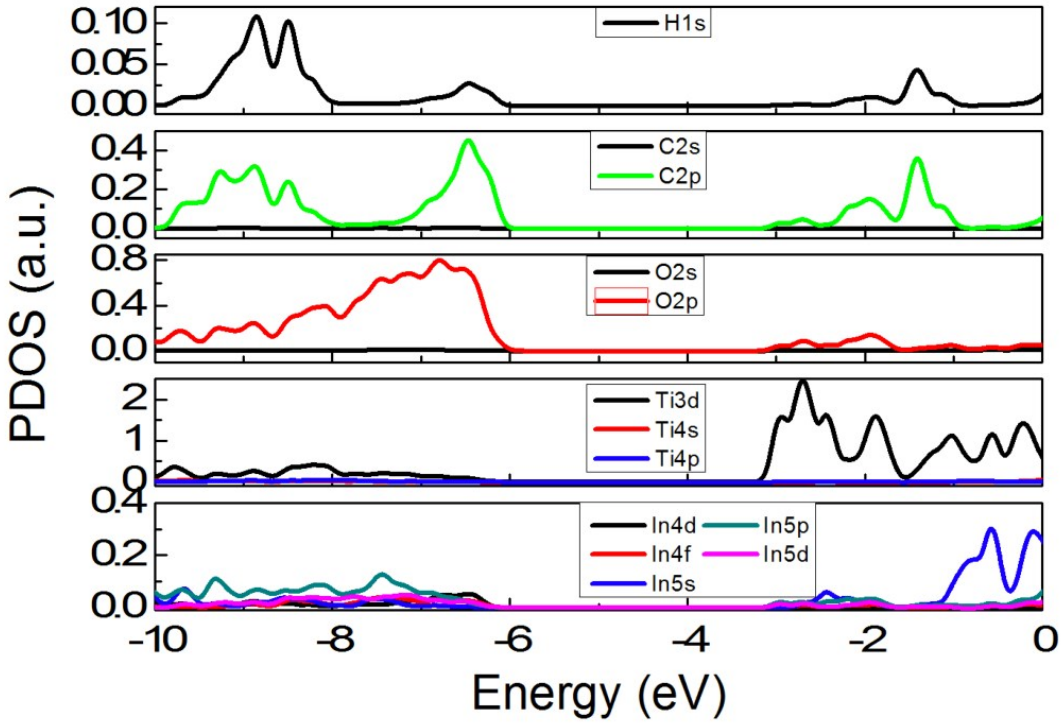

Fig. S15. Projected density of states (PDOS) per atom of **$POTi_{12}In_6$** cluster.

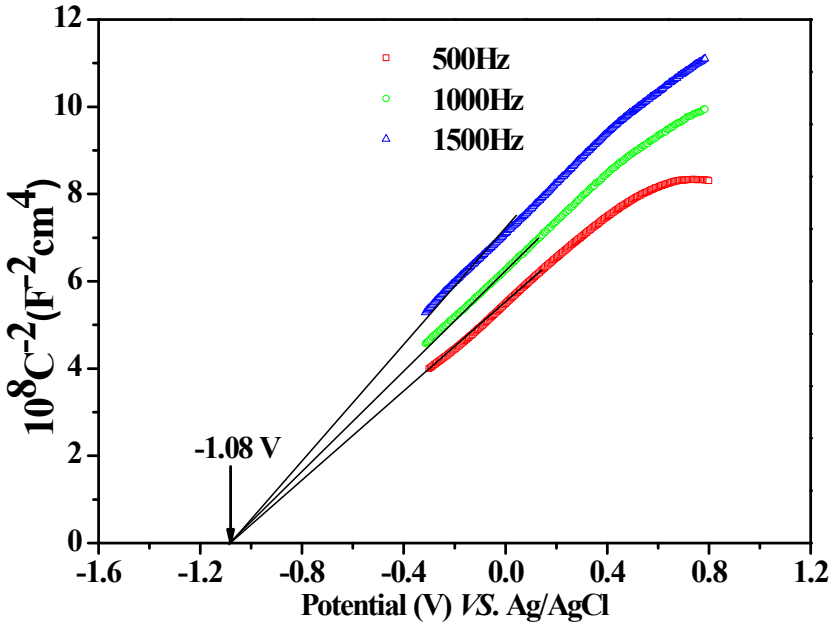

Fig. S16. Mott−Schottky plots for **$POTi_{12}In_6$** measured in 0.2 M Na_2SO_4 aqueous.

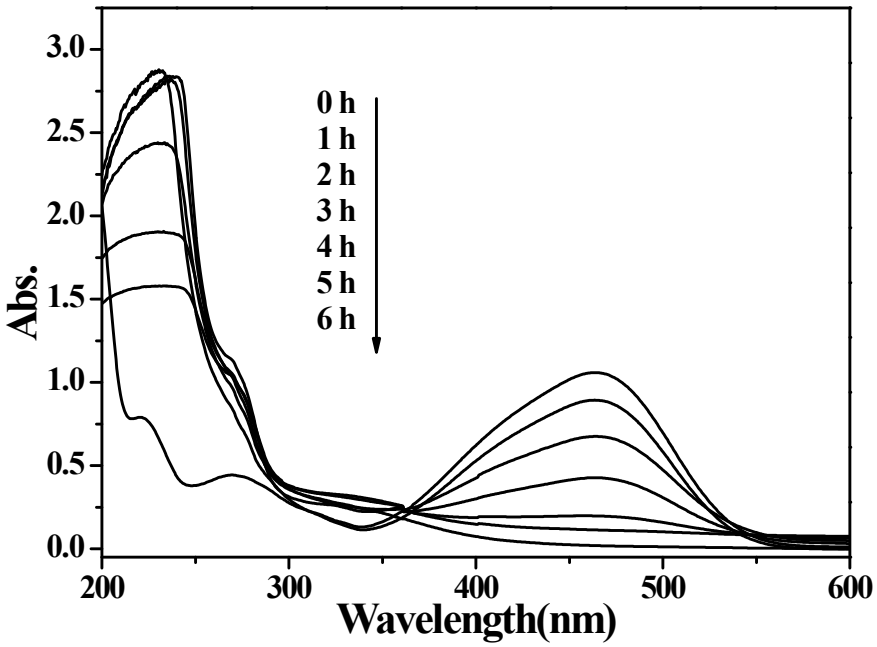

Fig. S17. UV-Visible spectroscopic changes for photodegrading methyl orange with **$POTi_{12}In_6$** (30 mg) and H_2O_2 (30%, 80uL) under visible irradiation.

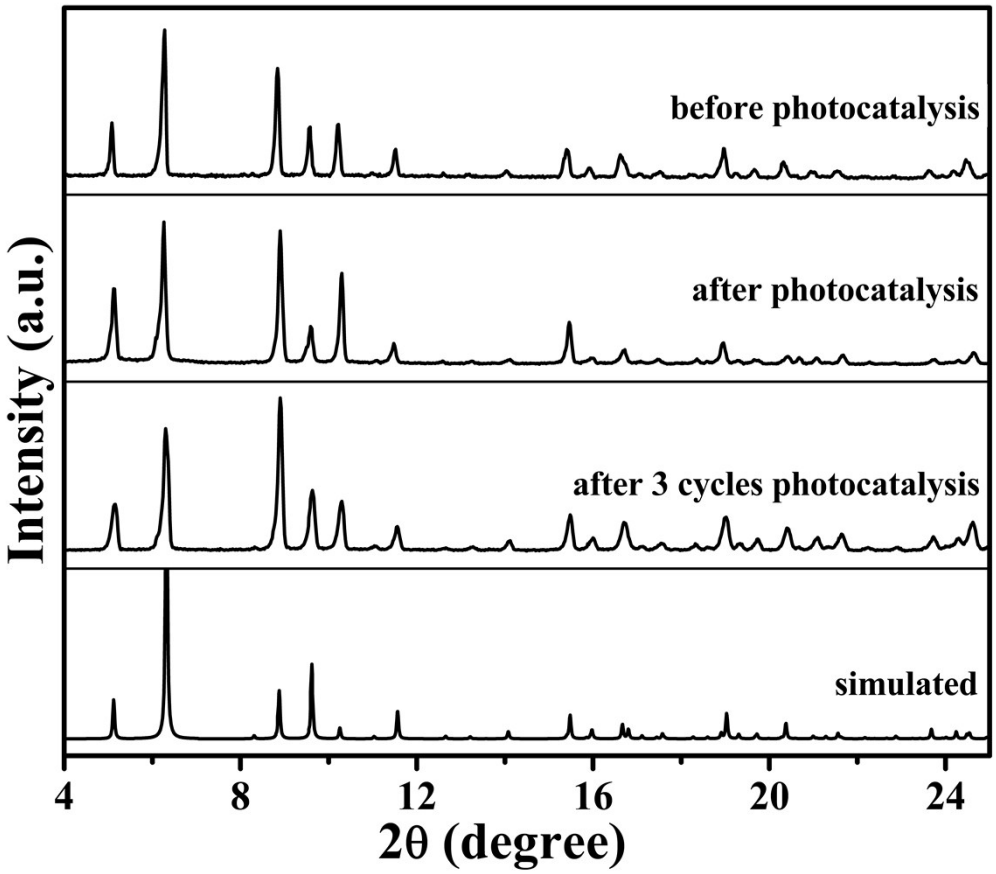

Fig. S18. Comparison of PXRD patterns of simulated $\mathbf{POTi_{12}In_6}$, $\mathbf{POTi_{12}In_6}$ before and after photocatalytic reaction (1 and 3 cycles), indicating crystalline structure of $\mathbf{POTi_{12}In_6}$ kept intact under photocatalytic conditions.

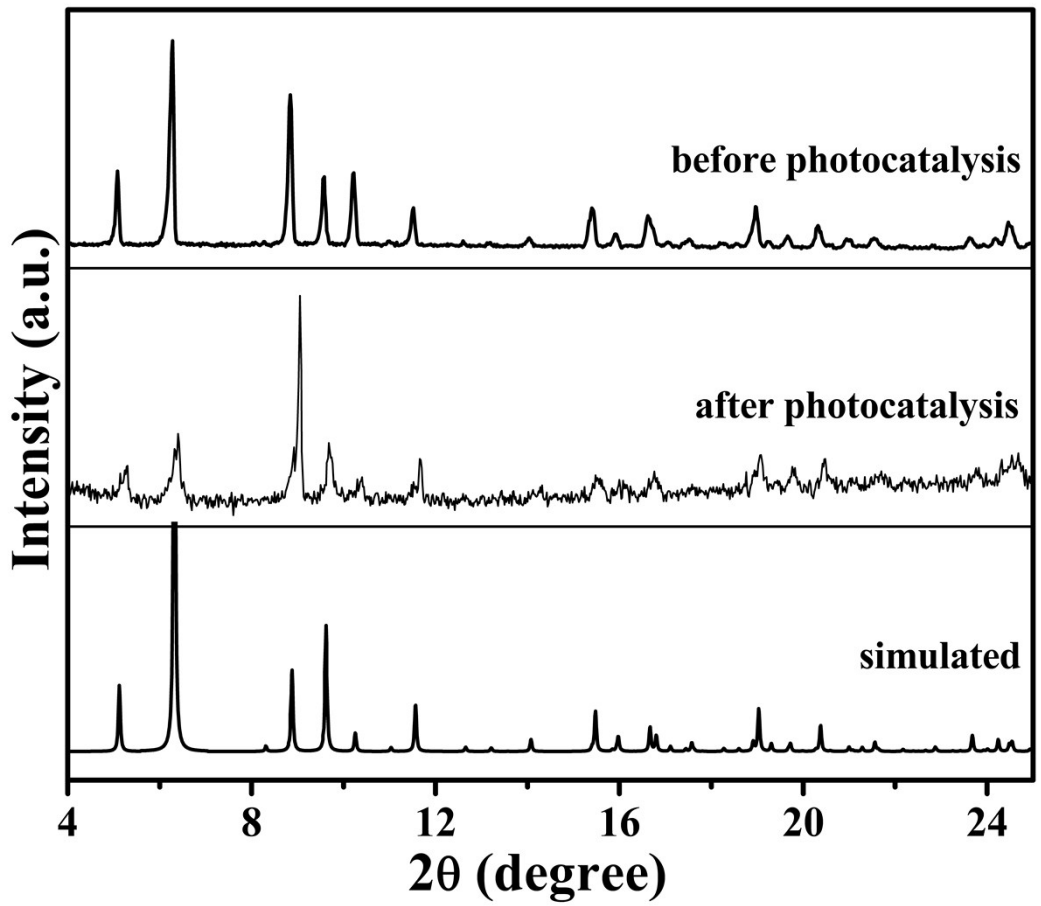

Fig. S19. The PXRD of simulated **$POTi_{12}In_6$**, **$POTi_{12}In_6$** before and after photocatalytic H_2 production.

References

1 T. Frot, S. Cochetet, G. Laurent, C. Sassoye, M. Popall, C. Sanchez and L. Rozes, *Eur. J. Inorg. Chem.,* 2010, **36**, 5650.